Stem Cell Reports
Report
OPEN ACCESS

Cell Replacement Therapy Improves Pathological Hallmarks in a Mouse Model of Leukodystrophy Vanishing White Matter

Stephanie Dooves,[1] Prisca S. Leferink,[1] Sander Krabbenborg,[1] Nicole Breeuwsma,[1] Saskia Bots,[1] Anne E.J. Hillen,[1] Gerbren Jacobs,[1] Marjo S. van der Knaap,[1,2] and Vivi M. Heine[1,3,*]

[1]Pediatric Neurology, Emma Children's Hospital, Amsterdam UMC, Vrije Universiteit Amsterdam, Amsterdam Neuroscience, 1081 HV Amsterdam, the Netherlands

[2]Department of Functional Genomics, Center for Neurogenomics and Cognitive Research, Amsterdam Neuroscience, Vrije Universiteit Amsterdam, 1081 HV Amsterdam, the Netherlands

[3]Department of Complex Trait Genetics, Center for Neurogenomics and Cognitive Research, Amsterdam Neuroscience, Vrije Universiteit Amsterdam, 1081 HV Amsterdam, the Netherlands

*Correspondence: vm.heine@vumc.nl

https://doi.org/10.1016/j.stemcr.2019.01.018

SUMMARY

Stem cell therapy has great prospects for brain white matter disorders, including the genetically determined disorders called leukodystrophies. We focus on the devastating leukodystrophy vanishing white matter (VWM). Patients with VWM show severe disability and early death, and treatment options are lacking. Previous studies showed successful cell replacement therapy in rodent models for myelin defects. However, proof-of-concept studies of allogeneic cell replacement in models representative of human leukodystrophies are lacking. We tested cell replacement in a mouse model representative of VWM. We transplanted different murine glial progenitor cell populations and showed improved pathological hallmarks and motor function. Improved mice showed a higher percentage of transplanted cells that differentiated into GFAP$^+$ astrocytes, suggesting best therapeutic prospects for replacement of astroglial lineage cells. This is a proof-of-concept study for cell transplantation in VWM and suggests that glial cell replacement therapy is a promising therapeutic strategy for leukodystrophy patients.

INTRODUCTION

Leukodystrophies are genetic disorders that affect the white matter of the brain. They form a group of many different, rare disorders, all characterized by neurological dysfunction leading to severe disability. While leukodystrophies are caused by mutations in genes expressed in different cell types, glial cells play a major role in disease pathology. Glia replacement therapy is seen as one of the promising treatment options for leukodystrophies (van der Knaap et al., 2016). The transplanted healthy glia are expected to compensate for the aberrant functioning of the host glia in the brains of leukodystrophy patients. Early studies showed myelin formation after transplantation with oligodendrocyte progenitor cells (OPCs) in myelin mutants or demyelinated lesions in rodents (Groves et al., 1993; Learish et al., 1999). Previous studies showed that transplantation of human glial progenitor cells (GPCs) in the shiverer mouse, a hypomyelinating mouse model, resulted in structurally normal myelin sheets and increased survival, with a rescue of the shiverer phenotype in about 20% of the animals (Windrem et al., 2008). Shiverer mice have a deletion of a large part of the *Mbp* gene, which codes for an essential myelin protein, and therefore do not produce functional myelin (Readhead and Hood, 1990). The shiverer mice are often used as a model for hypomyelinating leukodystrophies, although there are no patients known with hypomyelination due to *MBP* mutations. The first clinical trial transplanting human glia in patients with leukodystrophy Pelizaeus-Merzbacher disease (PMD) showed no major side effects, indicating that this treatment option is safe (Gupta et al., 2012). To allow new clinical trials with therapeutic effects, we need cell replacement studies in animal models that are representative of human leukodystrophy (Marteyn et al., 2016).

Here we present a proof of concept that glia replacement has a therapeutic effect on vanishing white matter (VWM). VWM is one of the more prevalent leukodystrophies, caused by recessive mutations in *EIF2B1-5* (Leegwater et al., 2001). It is a progressive disease with most often an early-childhood onset (van der Knaap et al., 2006). The brain white matter of VWM patients is diffusely abnormal and cavitated, and shows selectively affected oligodendrocytes and astrocytes (Bugiani et al., 2013). Currently no curative treatment is available for VWM. We transplanted murine GPCs in the neonatal brain of VWM mice (Dooves et al., 2016), which recapitulate the human disease with a shortened lifespan, ataxia, and affected glia. One-third of the transplanted animals showed significant pathological improvement, which was independently confirmed by discriminant analysis. Motor skills, as assessed by the time to cross the balance beam, also showed significant improvements in VWM mice after cell transplantation.

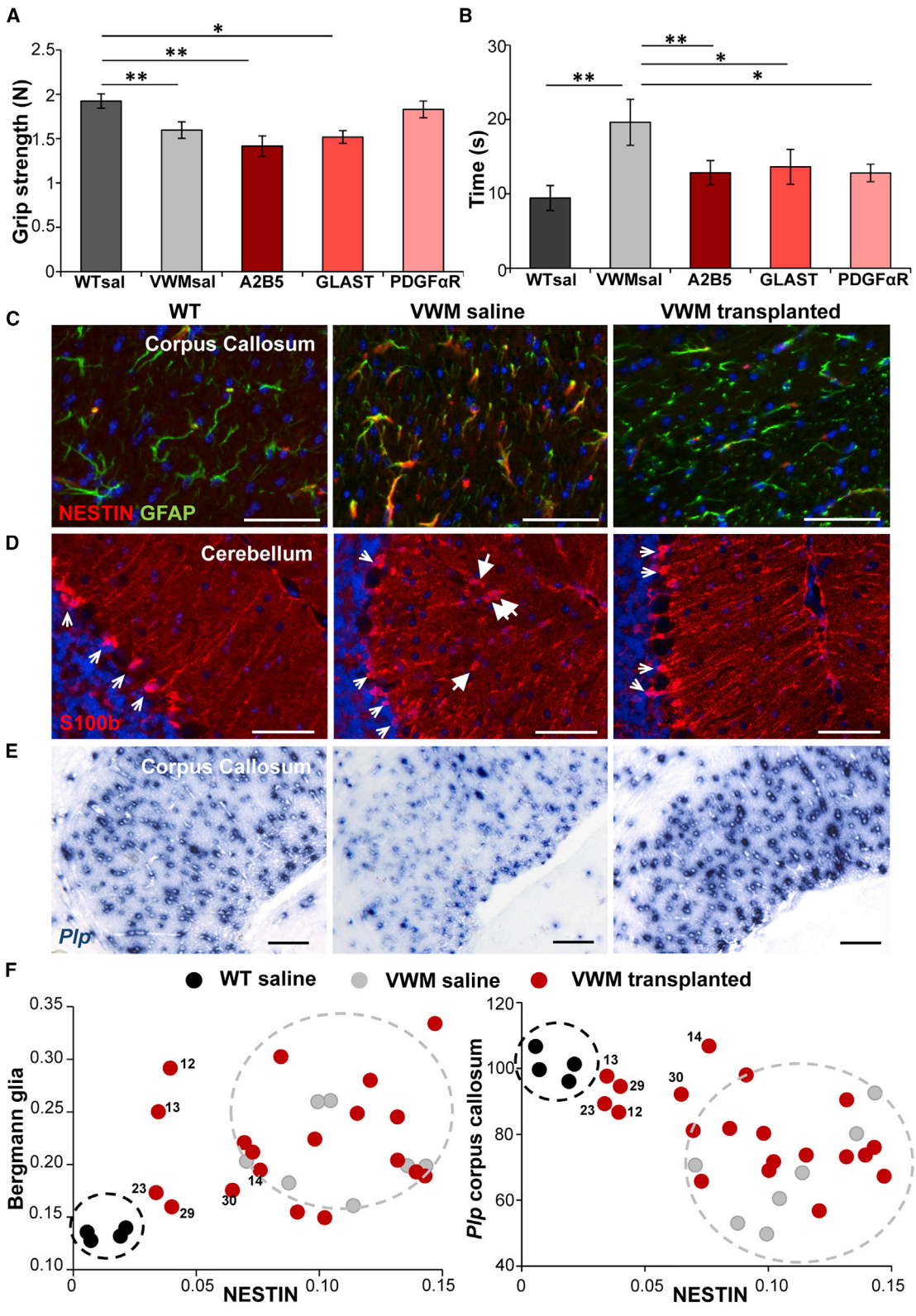

(legend on next page)

RESULTS

Motor Skills Were Improved after Transplantation

VWM mice (*2b5*^{ho}) were transplanted with either saline or primary mouse GPCs at postnatal day 0 (P0) at six injection sites, bilaterally in the anterior and posterior corpus callosum, and in the cerebellum. GPCs were sorted based on marker expression for A2B5 (mixed GPCs; Zhang et al., 2014), GLAST (astroglial lineage; Zhang et al., 2014), or PDGFαR (OPCs; Sim et al., 2011), and labeled with GFP before injection.

Previous studies showed that VWM mice show motor deficits (Dooves et al., 2016). We tested whether cell transplantation gave improved performance on the balance beam, grip strength, and footprint tests. No significant improvement was observed in the number of slips on the balance beam, in gait parameters, or on grip strength (Figure 1A). Interestingly, for all cell types the injected animals showed a significant improvement on the time to cross the balance beam (Figure 1B), indicating that cell transplantation led to functional improvement.

Transplantation Improved the Brain Pathology in a Subset of VWM Mice

VWM mice and patients are characterized by immature and abnormal astrocytes and oligodendrocytes in the white matter of the brain. We previously established that these pathological changes can be measured with three quantitative markers: (1) an increased number of NESTIN$^+$ astrocytes in the corpus callosum; (2) an increased number of translocated Bergmann glia in the cerebellum (from the Purkinje cell layer into the molecular layer); and (3) a decreased number of *Plp*-expressing oligodendrocytes in the corpus callosum and white matter of the cerebellum compared with control (Dooves et al., 2018). These VWM disease markers were assessed in the 9-month-old saline and cell-treated animals (Figures 1C–1E and S1A; Table S1). A number of cell-treated mice presented values on the pathological parameters that were more comparable with wild-type (WT) than with saline-treated VWM mice (Figures 1F and S1A; Table S1). To independently identify the improved VWM mice, we implemented a discriminant analysis. Optimal discriminant function parameters were determined using SPSS software based on scores on the pathology parameters in control groups: the saline-injected WT (WTsal) and VWM (VWMsal) mice. The discriminant function was applied to all transplanted animals and classified 6 out of 19 transplanted mice as "WT," indicating that these mice had scores on the disease markers that are more comparable with WTsal mice than VWMsal mice (Tables 1 and S1). Surprisingly, the GPC populations showed no obvious differences in improvement on the VWM disease parameters: all groups contained improved animals (improvement in 3 out of 8 A2B5$^+$, 1 out of 6 GLAST$^+$, 2 out of 5 PDGFαR$^+$ cell-injected mice). Thus cell transplantation led to improvements in the pathological hallmarks of VWM in a subset of mice, with no clear indications that a specific GPC population was better than the others.

Transplanted Primary Mouse Cells Survived and Integrated into Host Tissue

After transplantation, all GPC populations integrated into the host tissue (Figures 2A, S1B, and S1C). GFP-labeled donor cells were found in different brain areas of transplanted mice (Figure S1C). To study whether the *in vivo* microenvironment affected the fate of the donor cells, we analyzed the survival and cell fate of the grafted GPCs. After transplantation, all primary GPC populations differentiated into astrocytes and oligodendrocytes (Figures 2A and 2B). The A2B5$^+$ and PDGFαR$^+$ GPCs showed no significant changes in the percentage of OLIG2$^+$ and GFAP$^+$ donor cells over time. Although after injection of GLAST$^+$ GPCs, OLIG2$^+$ and GFAP$^+$ cells were present at all ages, their percentages showed a decrease between 2 and 9 months (OLIG2 2 months 39% 9 months 1%; GFAP

Figure 1. Improved VWM Pathology and Motor Dysfunction after Glial Cell Transplantation

(A) Strength of hind and front paws combined as measured on a grip strength meter in Newton. VWM saline (VWMsal) mice have significantly less strength in their paws compared with WT saline (WTsal) mice. This was similar for mice injected with A2B5$^+$ and GLAST$^+$ GPC populations. Mice that received PDGFαR$^+$ GPCs did not show significant differences with the VWMsal mice or WTsal mice.

(B) Time to cross the balance beam (in seconds) for all groups of mice. VWMsal mice were significantly slower than WTsal mice, but all cell-treated groups showed a significant improvement.

(C–E) Representative pictures of the VWM disease markers in WT, saline-treated, and cell-transplanted VWM mice (mouse 29) that showed improvement. (C) NESTIN and GFAP double staining in the corpus callosum. (D) S100β staining; big arrows show translocated Bergmann glia, small arrows show correctly located Bergmann glia. (E) *Plp in situ* hybridization.

(F) Quantification of the disease markers in all animals. Every data point represents an individual mouse. WT mice: n = 4, black; VWM saline mice: n = 7, gray; VWM transplanted mice: n = 19, red. The circles in black and gray illustrate the range of values of WT and saline VWM mice, respectively. In both plots a number of transplanted animals cluster more with the WT animals than with the saline-treated mice; these mice are indicated with numbers.

Graphs in (A) and (B) show mean of individual mice ± SEM. WTsal n = 36, VWMsal n = 31, A2B5 n = 9, GLAST n = 7, PDGFαR n = 6. *$p < 0.05$, **$p < 0.01$. Scale bars, 50 μm. See also Figure S1A.

Table 1. Discriminant Analysis Classifies One-Third of Transplanted Animals as WT

Mouse Number	Group[a]	Genotype[b]	Predicted Genotype[c]	Probability WT[d]
1	Saline	WT	WT	1.0000
2	Saline	WT	WT	1.0000
3	Saline	WT	WT	1.0000
4	Saline	WT	WT	1.0000
5	Saline	VWM	VWM	0.0000
6	Saline	VWM	VWM	0.0000
7	Saline	VWM	VWM	0.0000
8	Saline	VWM	VWM	0.0000
9	Saline	VWM	VWM	0.0000
10	Saline	VWM	VWM	0.0000
11	Saline	VWM	VWM	0.0000
12[e]	A2B5	VWM	WT	1.0000
13[e]	A2B5	VWM	WT	1.0000
14[e]	A2B5	VWM	WT	1.0000
15	A2B5	VWM	VWM	0.0000
16	A2B5	VWM	VWM	0.0000
17	A2B5	VWM	VWM	0.0000
18	A2B5	VWM	VWM	0.0004
19	A2B5	VWM	VWM	0.0003
20	GLAST	VWM	VWM	0.0005
21	GLAST	VWM	VWM	0.0000
22	GLAST	VWM	VWM	0.0246
23[e]	GLAST	VWM	WT	0.9998
24	GLAST	VWM	VWM	0.0000
25	GLAST	VWM	VWM	0.0000
26	PDGFαR	VWM	VWM	0.0000
27	PDGFαR	VWM	VWM	0.0000
28	PDGFαR	VWM	VWM	0.0000
29[e]	PDGFαR	VWM	WT	0.9999
30[e]	PDGFαR	VWM	WT	0.9992

See also Table S1.

[a]Saline = saline-injected mice; A2B5, GLAST, and PDGFαR = mice injected with primary mouse cells sorted on marker expression of the named proteins.

[b]Genotype of mice: WT, wild-type mice; VWM, vanishing white matter mice.

[c]Predicted genotype according to discriminant analysis.

[d]Probability of a mouse to have a WT genotype according to the discriminant analysis.

[e]Underlining indicates transplanted animals that were classified as WT in the discriminant analysis.

2 months 53%, 9 months 5%). No significant changes were observed in the glial fate between the different GPC populations after transplantation (Figure 2B).

To analyze differences in survival, we quantified the total number of engrafted cells at 2, 5, and 9 months for each cell population. About 40% of the injected cells survived and integrated into the host tissue (Figure 2C). No significant changes in cell survival were observed over time. However, the mice that received PDGFαR$^+$ cell injections showed a higher number of engrafted cells than mice that received A2B5$^+$ or GLAST$^+$ cell injections ($p < 0.001$; Figure 2C). Interestingly, the improved animals contained donor cell populations with a higher percentage GFAP$^+$ cells than the unimproved animals ($p = 0.04$, Figure 2D). Although not significantly different, improved mice showed a higher number of integrated cells in the corpus callosum and the cerebellum, areas important for VWM pathology (Figure 2E).

To conclude, after *in vivo* transplantations no differences in differentiation patterns between GPC populations are observed at 2, 5, or 9 months after cell transplantation, but the PDGFαR$^+$ GPC population showed a higher cell engraftment than the A2B5$^+$ or GLAST$^+$ GPC populations. In comparison with unimproved mice, the improved mice showed a higher percentage of engrafted cells that were GFAP$^+$.

GPC Populations Showed Minor Differences after *In Vitro* Maintenance

We performed a more detailed analysis on whether the performed cell sorting resulted in GPC populations with different properties. Cells were plated and analyzed by immunostaining at 1 day and 1 week after sorting (Figure 3). The A2B5$^+$ population showed a small (non-significant) increase in percentage of OLIG2$^+$ cells compared with the A2B5$^-$ population after sorting (Figures 3A and 3B). The GLAST$^+$ population showed a significantly increased percentage of astroglial lineage cells (GFAP$^+$ $p = 0.021$ and SOX9$^+$ $p = 0.021$) at 1 day after sorting (Figures 3C and 3D). At 1 week, significant differences between the GLAST$^+$ and GLAST$^-$ population were no longer observed. The PDGFαR$^+$ population showed a significantly increased percentage of PDGFαR$^+$ cells ($p = 0.05$) at day 1 after sorting compared with the PDGFαR$^-$ population; this percentage was diminished after 1 week in culture (Figures 3E and 3F).

In vitro qPCR analysis immediately after sorting showed that the GLAST$^+$ population expressed a higher amount of *Glast* ($p < 0.01$) than all other cell populations (Figure 3G). The PDGFαR$^+$ population had significantly higher

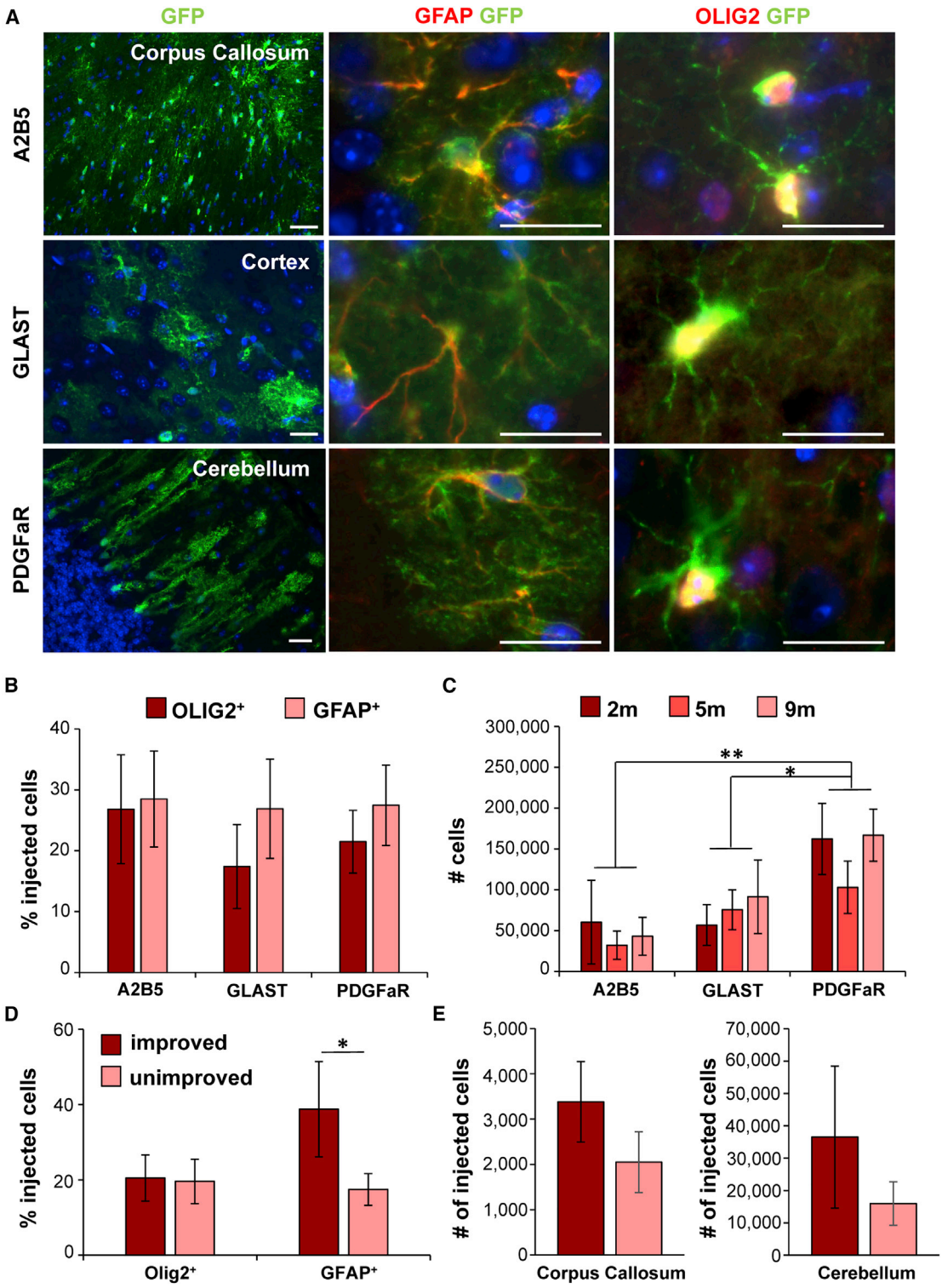

Figure 2. All GPC Populations Show Similar Glial Fate *In Vivo* while Improved Mice Show Increased Astrocytic Differentiation

(A) After transplantations, all GPCs integrated into various brain areas (left) and were capable of differentiating into astrocytes (middle) and oligodendrocytes (right).

(B) Analysis of cell fate showed that cells from all GPC populations differentiated into GFAP$^+$ astrocytes and OLIG2$^+$ oligodendrocytes.

(legend continued on next page)

expression of *Olig2* ($p < 0.001$) and *Pdgfra* ($p < 0.001$) than all other cell populations (Figure 3G).

Earlier studies suggested that regenerative properties of transplanted cells are mediated via secretion of trophic factors (Hawryluk et al., 2012; Pluchino et al., 2009). To identify trophic factor secretion in GPC populations, we studied RNA expression levels of *Ngf1*, *Nt3*, *Pdgfa*, *Egf*, *Lif*, *Igf1*, and *Tgfb* immediately after sorting. All cell populations expressed all factors with only subtle differences (Figure S2). Significant differences were only observed for the GLAST$^+$ population, which showed a significantly increased expression of *Igf1* ($p < 0.05$; Figure S2) and a significantly decreased expression of *Ngf1* ($p < 0.01$; Figure S2).

While cell sorting was aimed to create GPC populations with diverse differentiation potentials, *in vitro* analysis showed that over time all populations developed into astrocytic and oligodendrocytic lineage cells and expressed trophic factors with only minor differences.

DISCUSSION

This study shows that neonatal transplantation with GPCs can improve motor skills and the pathology of a mouse model representative of human leukodystrophy VWM. We show that mouse glia, which lack the phylogenetic advantage of human glia, successfully integrate into the host tissue and differentiate into astrocytes and oligodendrocytes. All GPC populations engrafted well, differentiated into astrocytic and oligodendrocytic lineage cells, and were able to improve the VWM phenotype. However, mice that received PDGFaR$^+$ cells showed the highest number of engrafted cells. The mice that showed improvements in pathology had a higher percentage of engrafted cells that differentiated into GFAP$^+$ astrocytes, which was independent of the engrafted GPC population. This suggests that the mechanisms underlying recovery are dependent on astrocytes and that transplantation with a highly astrogenic progenitor population is important. This latter finding is in agreement with a previous study showing an important role for astrocytes in VWM pathology (Dooves et al., 2016), and further suggests that astrocyte replacement has the best therapeutic prospects for VWM.

In this study we used a discriminant analysis to classify transplanted mice into a "WT" or "VWM" phenotype. For treatments that show a large variability in their effects and with small sample sizes, this is a useful tool to identify individual mice or patients that show improvement of their symptoms, even though the means of the treatment groups are not significantly improved (Shayan et al., 2015). We showed that one-third of the transplanted mice showed pathological improvements after cell transplantation, which is consistent with previous studies that transplanted human cells in rodent models of myelin defects (Uchida et al., 2012; Windrem et al., 2008). So far glia transplantations with mouse cells (Lyczek et al., 2017) in models representative of human leukodystrophies have been more challenging. Rodent astrocytes are markedly different from human astrocytes (Oberheim et al., 2009) and lack the phylogenetic advantage that human cells have when transplanted into a rodent model. After neonatal transplantation in mice, human GPCs are able to outcompete their rodent counterparts, leading to mice with essentially a humanized white matter (Windrem et al., 2014). As human glia also do not have a phylogenetic advantage when transplanted in patients, we considered it important to prove recovery after transplanting mouse GPCs into VWM mice.

The therapeutic effects of cell transplants could be improved by changing treatment strategies. First, most leukodystrophies have a complex pathophysiology involving multiple cell types and toxic microenvironments. For example, OPC transplantation in Krabbe disease failed, probably due to the accumulation of psychosine in the microenvironment, which is toxic for mature oligodendrocytes Kuai et al. (2015). A recent study showed that transplantations with human neural precursor cells in a transgenic mouse model for PMD gave better improvements than transplantation with human OPCs, while human OPCs gave better improvements in shiverer mice (Marteyn et al., 2016). This highlights the influence of the microenvironment that is distinct to each disease and the importance of testing specific cell types in appropriate disease models. We showed that all GPC populations expressed trophic factors in comparable amounts. As trophic factors can have an influence on the brain microenvironment (Hawryluk et al., 2012), all animals could have been affected by GPC-secreted factors. The effect of neurotrophic factors on the VWM microenvironment is beyond the scope of this article but is an interesting topic for future studies.

Earlier studies showed that the VWM microenvironment has increased hyaluronan levels (Bugiani et al., 2013;

(C) The number of donor cells was similar in 2-, 5-, and 9-month-old mice. The survival of PDGFαR$^+$ cells after transplantation was significantly increased compared with A2B5$^+$ and GLAST$^+$ cells.
(D) Improved mice had a significantly higher percentage of injected cells (GFP$^+$) that were GFAP$^+$ compared with unimproved mice.
(E) Improved mice showed a higher average number of donor cells present in the corpus callosum and cerebellum, albeit not significantly.
In (B) and (C), A2B5$^+$ n = 13 mice; GLAST$^+$ n = 10 mice; PDGFαR$^+$ n = 17 mice. In (D) and (E), improved n = 6 mice; unimproved n = 18 mice.
(B) to (E) show mean ± SEM; *$p < 0.05$, **$p < 0.01$. Scale bars, 20 μm. See also Figures S1B and S1C.

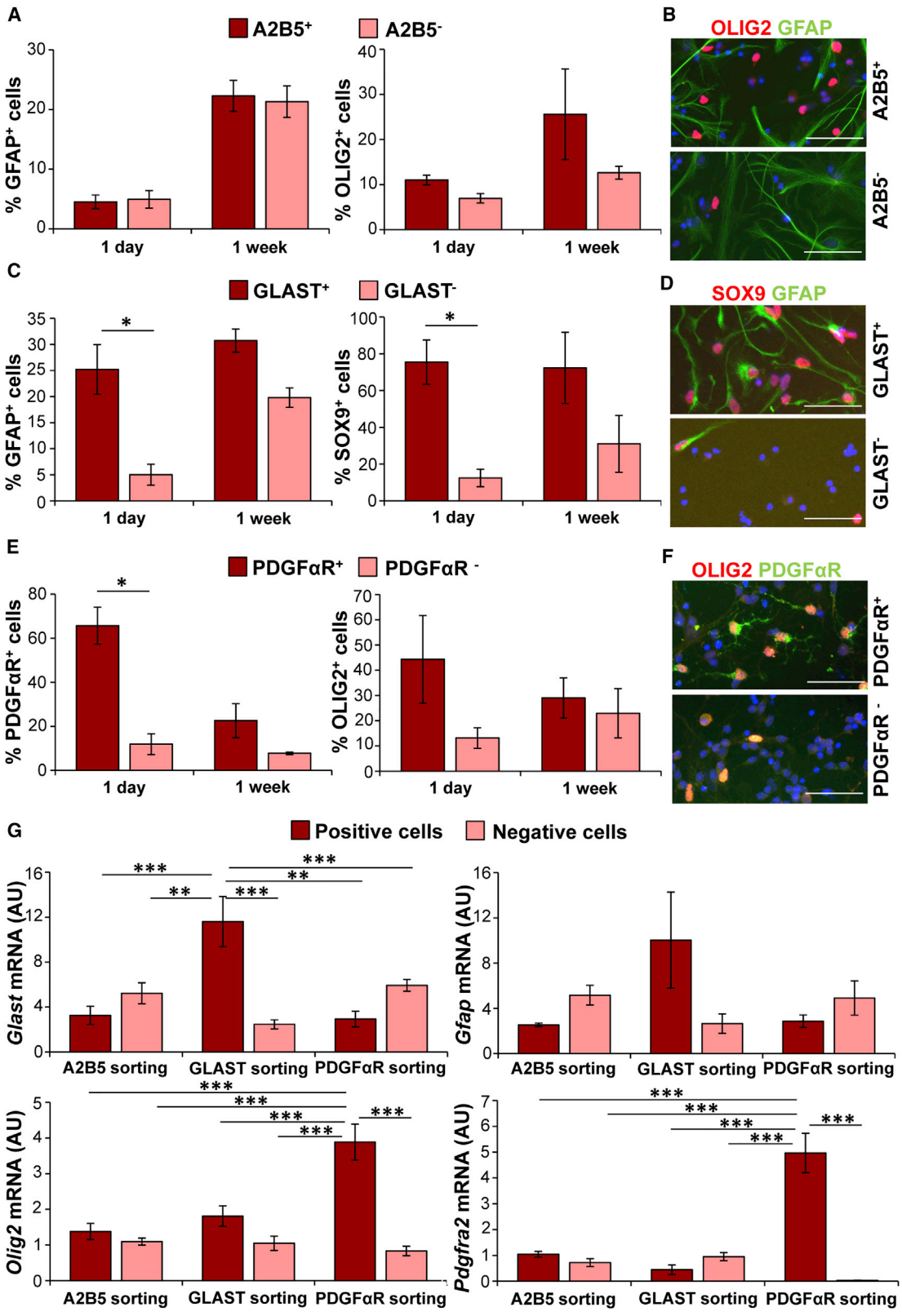

(legend on next page)

Dooves et al., 2016). As hyaluronan can impede oligodendrocyte maturation (Back et al., 2005), this could be a complicating factor in cell replacement therapy. The current study may have benefited from neonatal transplantations, as no pathology or increased hyaluronan level is observed at that age. Cell transplantations in patients will likely benefit from modulation of the microenvironment by, for example, using drugs that make the microenvironment less hostile for donor cells. Second, injection of neonatal mice with high precision is challenging and induces variability due to the number of surviving cells, the injection location, and the cell fate. For the study of how transplantation parameters and a symptomatic VWM environment affect survival and integration of donor cells, transplantations at a later age could be considered.

For clinical trials we need cell populations that have therapeutic effects and are safe for use in humans. With the discovery of induced pluripotent stem cells (iPSCs) in 2006 (Takahashi and Yamanaka, 2006) and current advantages in gene correction methods (Maeder and Gersbach, 2016), it is possible to make genetically corrected patient-specific iPSC-derived glia, limiting the risk of rejection. *In vitro* disease modeling with patient iPSCs allows the study of how different mutations affect disease mechanisms (Nevin et al., 2017; Numasawa-Kuroiwa et al., 2014) and human-specific disease aspects. Different studies have shown that iPSC-derived GPCs have potential for white matter repair similarly to GPCs derived from fetal tissue of embryonic stem cells (Ehrlich et al., 2017; Wang et al., 2013). Recently, a clinical study using iPSC-derived cells for macular degeneration showed no tumor formation of the injected cells (Mandai et al., 2017), showing promise for the use of iPSCs in clinical applications.

To conclude, this study demonstrates the potential of cell transplantation for VWM, and shows the efficacy of allogeneic murine cell transplantation in a rodent model for a specific leukodystrophy. Although more research is needed to optimize transplantation parameters, the positive results indicate that stem cell transplantation is a promising therapeutic option for leukodystrophies such as VWM.

EXPERIMENTAL PROCEDURES

Cell Injections

Cells were sorted on marker expression of A2B5, GLAST, or PDGFαR with magnetic-activated cell sorting (MACS) according to the manufacturer's protocol. WT and VWM mice were injected at postnatal day 0 (P0) with sorted cells labeled with GFP virus. At 7 months of age the motor skills of all mice were tested. Brain tissue was collected at 2, 5, and 9 months of age, and used for analysis of cell fate, cell survival, and improvement of pathology. All mouse procedures were carried out according to the guidelines of the Dutch government and approved by the Animal Approval Committee of the VU University, Amsterdam. See Supplemental Experimental Procedures for more details.

In Vitro Cell Analysis

After MACS, cells were either directly used to extract RNA or plated on 8-well chamberslides for immunostaining. RNA was analyzed by qPCR markers for cell fate and neurotrophic factors. Cells that were plated on chamberslides were fixed 1 day and 1 week after sorting. Immunostaining was used to analyze cell fate. See Supplemental Experimental Procedures for more details.

Statistical Analysis

All data were analyzed using SPSS software (IBM SPSS Statistics 20.0). All data were tested for normal distribution and appropriate statistical tests chosen. See Supplemental Experimental Procedures for more details.

SUPPLEMENTAL INFORMATION

Supplemental Information includes Supplemental Experimental Procedures, two figures, and two tables and can be found with this article online at https://doi.org/10.1016/j.stemcr.2019.01.018.

Figure 3. Sorted GPCs Show Different Identity after Short-Term Maintenance *In Vitro*

Primary cells were sorted by MACS for marker expression of A2B5, GLAST, or PDGFαR.

(A–F) Immunostaining of cells from positive selection and cells that were not bound to microbeads ("negative") after 1 day and 1 week in culture. (A and B) $A2B5^+$ and $A2B5^-$ population both are positive for GFAP and OLIG2. (C and D) $GLAST^+$ population showed a significantly higher percentage of cells that were positive for astrocyte markers GFAP and SOX9 at 1 day after sorting compared with the $GLAST^-$ population. After 1 week in culture there are no longer significant differences. (E and F) $PDGF\alpha R^+$ population showed a significantly higher percentage of cells that are positive for PDGFαR, and an increased number of cells positive for OLIG2, compared with the $PDGF\alpha R^-$ population. After 1 week in culture no significant differences are observed.

(G) A qPCR analysis shows that $GLAST^+$ population has a higher expression of *Glast*, and $PDGF\alpha R^+$ population shows a higher expression of *Olig2* and *Pdgfra* than any of the other conditions.

Error bars represent mean ± SEM. n = 3 independent sortings for all. *p < 0.05, **p < 0.01, ***p < 0.001. (A), (C), and (E) show percentages of positive cells compared with total number of $DAPI^+$ cells. (B), (D), and (F) show examples of immunostainings used for cell counts of cells at 1 day after plating. (G) shows $2^{\Delta Ct}$ values of qPCR analysis in arbitrary units (AU). Scale bars, 50 μm. See also Figure S2.

AUTHOR CONTRIBUTIONS

S.D. performed all experiments and analysis. S.K., N.B., S.B., P.S.L., and A.E.J.H. assisted in tissue slicing and immunostainings. G.J. assisted in virus production, cell culture, and genotyping of mice. S.D. and V.M.H. designed the study. S.D. and V.M.H. wrote the article with valuable contributions of M.S.v.d.K.

ACKNOWLEDGMENTS

This study was financially supported by the NWO Spinoza grant (M.S.v.d.K.), ZonMw VIDI research grant 91712343 (V.M.H.), the ZonMw TAS IDB project 116005006 (V.M.H.), E-Rare Joint Call project 9003037601 (V.M.H., M.S.v.d.K.), and KNAW Ter Meulen Fonds (S.D.). We thank Paulien Cornelissen for technical assistance.

Received: September 12, 2017
Revised: January 18, 2019
Accepted: January 21, 2019
Published: February 21, 2019

REFERENCES

Back, S.A., Tuohy, T.M., Chen, H., Wallingford, N., Craig, A., Struve, J., Luo, N.L., Banine, F., Liu, Y., Chang, A., et al. (2005). Hyaluronan accumulates in demyelinated lesions and inhibits oligodendrocyte progenitor maturation. Nat. Med. *11*, 966–972.

Bugiani, M., Postma, N., Polder, E., Dieleman, N., Scheffer, P.G., Sim, F.J., van der Knaap, M.S., and Boor, I. (2013). Hyaluronan accumulation and arrested oligodendrocyte progenitor maturation in vanishing white matter disease. Brain *136*, 209–222.

Dooves, S., Bugiani, M., Postma, N.L., Polder, E., Land, N., Horan, S.T., van Deijk, A.L., van de Kreeke, A., Jacobs, G., Vuong, C., et al. (2016). Astrocytes are central in the pathomechanisms of vanishing white matter. J. Clin. Invest. *126*, 1512–1524.

Dooves, S., Bugiani, M., Wisse, L.E., Abbink, T.E.M., van der Knaap, M.S., and Heine, V.M. (2018). Bergmann glia translocation: a new disease marker for vanishing white matter identifies therapeutic effects of Guanabenz treatment. Neuropathol. Appl. Neurobiol. *44*, 391–403.

Ehrlich, M., Mozafari, S., Glatza, M., Starost, L., Velychko, S., Hallmann, A.L., Cui, Q.L., Schambach, A., Kim, K.P., Bachelin, C., et al. (2017). Rapid and efficient generation of oligodendrocytes from human induced pluripotent stem cells using transcription factors. Proc. Natl. Acad. Sci. U S A *114*, E2243–E2252.

Groves, A.K., Barnett, S.C., Franklin, R.J., Crang, A.J., Mayer, M., Blakemore, W.F., and Noble, M. (1993). Repair of demyelinated lesions by transplantation of purified O-2A progenitor cells. Nature *362*, 453–455.

Gupta, N., Henry, R.G., Strober, J., Kang, S.M., Lim, D.A., Bucci, M., Caverzasi, E., Gaetano, L., Mandelli, M.L., Ryan, T., et al. (2012). Neural stem cell engraftment and myelination in the human brain. Sci. Transl. Med. *4*, 155ra137.

Hawryluk, G.W., Mothe, A., Wang, J., Wang, S., Tator, C., and Fehlings, M.G. (2012). An in vivo characterization of trophic factor production following neural precursor cell or bone marrow stromal cell transplantation for spinal cord injury. Stem Cells Dev. *21*, 2222–2238.

Kuai, X.L., Ni, R.Z., Zhou, G.X., Mao, Z.B., Zhang, J.F., Yi, N., Liu, Z.X., Shao, N., Ni, W.K., and Wang, Z.W. (2015). Transplantation of mouse embryonic stem-cell derived oligodendrocytes in the murine model of globoid cell leukodystrophy. Stem Cell Res. Ther. *6*, 30.

Learish, R.D., Brustle, O., Zhang, S.C., and Duncan, I.D. (1999). Intraventricular transplantation of oligodendrocyte progenitors into a fetal myelin mutant results in widespread formation of myelin. Ann. Neurol. *46*, 716–722.

Leegwater, P.A.J., Vermeulen, G., Könst, A.A.M., Naidu, S., Mulders, J., Visser, A., Kersbergen, P., Mobach, D., Fonds, D., van Berkel, C.G.M., et al. (2001). Subunits of the translation initiation factor eIF2B are mutant in leukoencephalopathy with vanishing white matter. Nat. Genet. *29*, 383–388.

Lyczek, A., Arnold, A., Zhang, J., Campanelli, J.T., Janowski, M., Bulte, J.W., and Walczak, P. (2017). Transplanted human glial-restricted progenitors can rescue the survival of dysmyelinated mice independent of the production of mature, compact myelin. Exp. Neurol. *291*, 74–86.

Maeder, M.L., and Gersbach, C.A. (2016). Genome-editing technologies for gene and cell therapy. Mol. Ther. *24*, 430–446.

Mandai, M., Watanabe, A., Kurimoto, Y., Hirami, Y., Morinaga, C., Daimon, T., Fujihara, M., Akimaru, H., Sakai, N., Shibata, Y., et al. (2017). Autologous induced stem-cell- derived retinal cells for macular degeneration. N. Engl. J. Med. *376*, 1038–1046.

Marteyn, A., Sarrazin, N., Yan, J., Bachelin, C., Deboux, C., Santin, M.D., Gressens, P., Zujovic, V., and Baron-Van Evercooren, A. (2016). Modulation of the innate immune response by human neural precursors prevails over oligodendrocyte progenitor remyelination to rescue a severe model of Pelizaeus-Merzbacher disease. Stem Cells *34*, 984–996.

Nevin, Z.S., Factor, D.C., Karl, R.T., Douvaras, P., Laukka, J., Windrem, M.S., Goldman, S.A., Fossati, V., Hobson, G.M., and Tesar, P.J. (2017). Modeling the mutational and phenotypic landscapes of Pelizaeus-Merzbacher disease with human iPSC-derived oligodendrocytes. Am. J. Hum. Genet. *100*, 617–634.

Numasawa-Kuroiwa, Y., Okada, Y., Shibata, S., Kishi, N., Akamatsu, W., Shoji, M., Nakanishi, A., Oyama, M., Osaka, H., Inoue, K., et al. (2014). Involvement of ER stress in dysmyelination of Pelizaeus-Merzbacher disease with PLP1 missense mutations shown by iPSC-derived oligodendrocytes. Stem Cell Reports *2*, 648–661.

Oberheim, N.A., Takano, T., Han, X., He, W., Lin, J.H., Wang, F., Xu, Q., Wyatt, J.D., Pilcher, W., Ojemann, J.G., et al. (2009). Uniquely hominid features of adult human astrocytes. J. Neurosci. *29*, 3276–3287.

Pluchino, S., Gritti, A., Blezer, E., Amadio, S., Brambilla, E., Borsellino, G., Cossetti, C., Del Carro, U., Comi, G., 't Hart, B., et al. (2009). Human neural stem cells ameliorate autoimmune encephalomyelitis in non-human primates. Ann. Neurol. *66*, 343–354.

Readhead, C., and Hood, L. (1990). The dysmyelinating mouse mutations shiverer (shi) and myelin deficient (shi^{mld}). Behav. Genet. *20*, 213–234.

Shayan, Z., Mohammad Gholi Mezerji, N., Shayan, L., and Naseri, P. (2015). Prediction of depression in cancer patients with different classification criteria, linear discriminant analysis versus logistic regression. Glob. J. Health Sci. *8*, 41–46.

Sim, F.J., McClain, C.R., Schanz, S.J., Protack, T.L., Windrem, M.S., and Goldman, S.A. (2011). CD140a identifies a population of highly myelinogenic, migration-competent and efficiently engrafting human oligodendrocyte progenitor cells. Nat. Biotechnol. *29*, 934–941.

Takahashi, K., and Yamanaka, S. (2006). Induction of pluripotent stem cells from mouse embryonic and adult fibroblast cultures by defined factors. Cell *126*, 663–676.

Uchida, N., Chen, K., Dohse, M., Hansen, K.D., Dean, J., Buser, J.R., Riddle, A., Beardsley, D.J., Wan, Y., Gong, X., et al. (2012). Human neural stem cells induce functional myelination in mice with severe dysmyelination. Sci. Transl. Med. *4*, 155ra136.

van der Knaap, M.S., Pronk, J.C., and Scheper, G.C. (2006). Vanishing white matter disease. Lancet Neurol. *5*, 413–423.

van der Knaap, M.S., Wolf, N.I., and Heine, V.M. (2016). Leukodystrophies: five new things. Neurol. Clin. Pract. https://doi.org/10.1212/CPJ.0000000000000289.

Wang, S., Bater, J., Li, X., Schanz, S., Chandler-Militello, D., Levine, C., Maherali, N., Studer, L., Hochedlinger, K., Windrem, M., et al. (2013). Human iPSC-derived oligodendrocyte progenitor cells can myelinate and rescue a mouse model of congenital hypomyelination. Cell Stem Cell *12*, 252–264.

Windrem, M.S., Schanz, S.J., Guo, M., Tian, G.F., Washco, V., Stanwoord, N., Rasband, M., Roy, N.S., Nedergaard, M., Havton, L.A., et al. (2008). Neonatal chimerization with human glial progenitor cells can both remyelinate and rescue the otherwise lethally hypomyelinated shiverer mouse. Cell Stem Cell *2*, 553–565.

Windrem, M.S., Schanz, S.J., Morrow, C., Munir, J., Chandler-Militello, D., Wang, S., and Goldman, S.A. (2014). A competitive advantage by neonatally engrafted human glial progenitors yields mice whose brain are chimeric for human glia. J. Neurosci. *34*, 16153–16161.

Zhang, Y., Chen, K., Sloan, S.A., Bennett, M.L., Scholze, A.R., O'Keeffe, S., Phatnani, H.P., Guarnieri, P., Caneda, C., Ruderisch, N., et al. (2014). An RNA-sequencing transcriptome and splicing database of glia, neurons, and vascular cells of the cerebral cortex. J. Neurosci. *34*, 11929–11947.

Stem Cell Reports, Volume *12*

Supplemental Information

Cell Replacement Therapy Improves Pathological Hallmarks in a Mouse Model of Leukodystrophy Vanishing White Matter

Stephanie Dooves, Prisca S. Leferink, Sander Krabbenborg, Nicole Breeuwsma, Saskia Bots, Anne E.J. Hillen, Gerbren Jacobs, Marjo S. van der Knaap, and Vivi M. Heine

Supplemental Figures

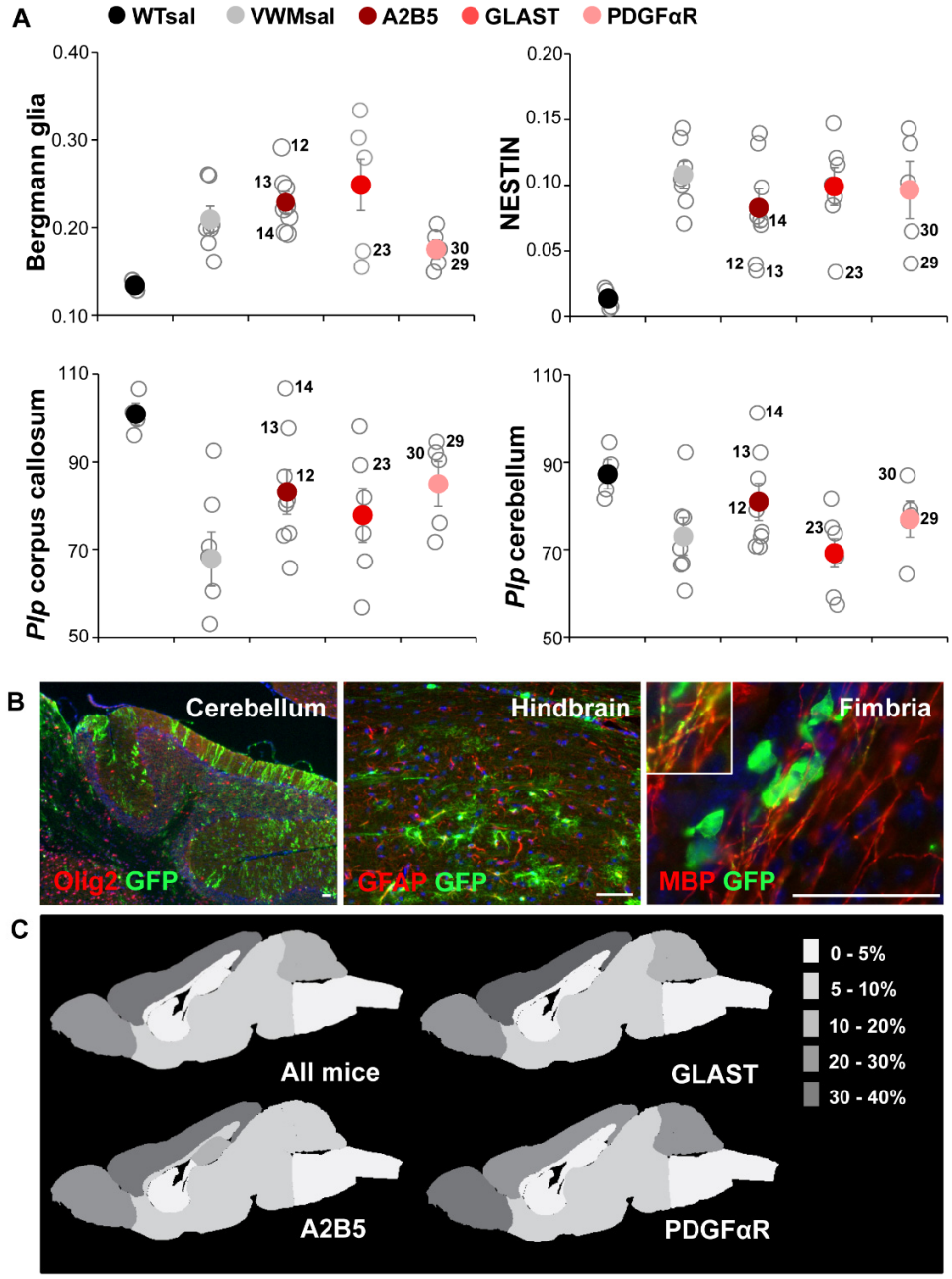

Figure S1. Pathology scores and cell dispersal after transplantation. Related to Figure 1 and 2. (A) shows the data of all mice on the three disease markers: Bergmann glia translocation (left top), the number of NESTIN$^+$ astrocytes in the corpus callosum (right top), and the number of *Plp*$^+$ oligodendrocytes in the corpus callosum (left bottom) and cerebellum (right bottom). Open data points indicate individual mice, with solid data points indicating group means ± SEM. The animals that showed improvement according to the discriminant analysis are indicated by numbers. WTsal = WT saline injected mice n=4, VWMsal = VWM saline injected mice n=7, A2B5 = VWM A2B5$^+$ cells injected mice n=8, GLAST = VWM GLAST$^+$ cells injected mice n=6, PDGFαR = VWM PDGFαR$^+$ cells injected mice n=5. (B) shows that injected (GFP$^+$) cells have migrated to different brain areas such as the cerebellum, hindbrain or fimbria. (C) shows the percentage of the total number of injected cells that have migrated to a specific

brain region, to give an overview of cell dispersal. The percentages are calculated for all mice (left top; n=40 mice) and separately for mice that received A2B5^{+} (left bottom; n=13 mice), GLAST^{+} (right top; n=10 mice) or PDGFαR^{+} (right bottom; n=17 mice) cell injections. Note that although white matter areas as the corpus callosum did not receive a high percentage of the total injected cells, the corpus callosum is also a much smaller area than for example the cortex which has not been taken into account in these calculations. Scalebars = 50 µm.

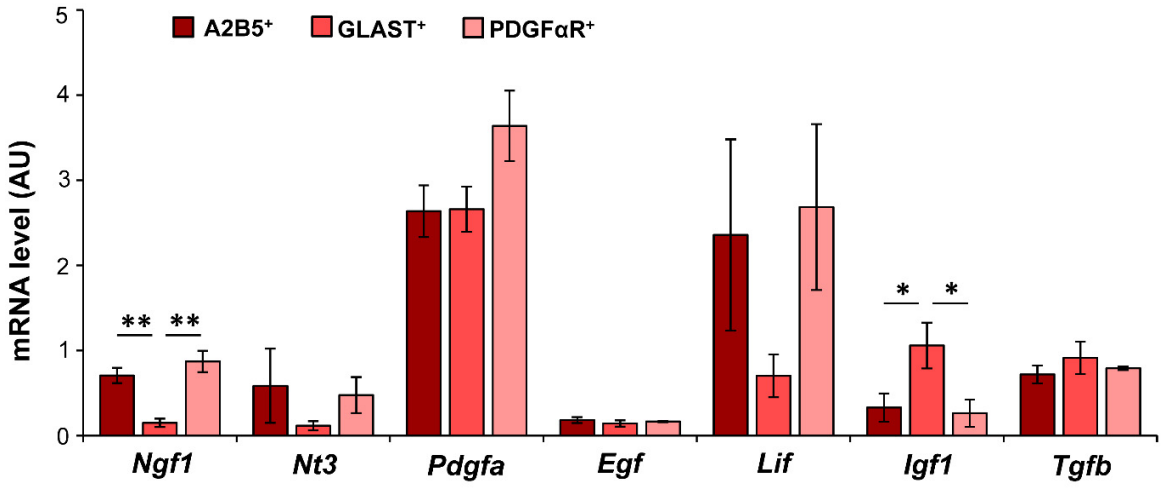

Figure S2. In vitro analysis of GPCs. Related to Figure 3. mRNA levels of neurotrophic factors in A2B5^{+}, GLAST^{+} and PDGFαR^{+}, based on qPCR analysis of 3 independent experiments. Only minor differences between GPC populations are observed, with a significant decrease of *Ngf1* and a significant increase of *Igf1* in the GLAST^{+} cells. Bars represent mean ± SEM. Shown are $2^{-\Delta CT}$ values in arbitrary units (AU). N=3 independent sortings for all. * = $p<.05$, ** = $p<.01$

Table S1. All pathology data. Related to Table 1.

Mouse#	Group[a]	Genotype[b]	Gender	Nestin[c]	BG[d]	*Plp* cc[e]	*Plp* cer[f]
1	Saline	WT	M	0.021	0.140	101	82
2	Saline	WT	M	0.019	0.132	96	84
3	Saline	WT	M	0.006	0.136	107	90
4	Saline	WT	M	0.007	0.128	100	95
5	Saline	VWM	M	0.136	0.199	80	77
6	Saline	VWM	M	0.105	0.261	60	61
7	Saline	VWM	M	0.099	0.260	50	67
8	Saline	VWM	M	0.143	0.198	93	92
9	Saline	VWM	F	0.070	0.203	71	67
10	Saline	VWM	F	0.114	0.161	68	70
11	Saline	VWM	F	0.088	0.182	53	78
12[g]	**A2B5**	**VWM**	**F**	**0.039**	**0.291**	**87**	**79**
13[g]	**A2B5**	**VWM**	**F**	**0.035**	**0.250**	**98**	**92**
14[g]	**A2B5**	**VWM**	**F**	**0.076**	**0.195**	**107**	**101**
15	A2B5	VWM	F	0.132	0.245	73	71
16	A2B5	VWM	M	0.139	0.193	74	73
17	A2B5	VWM	M	0.073	0.212	66	74
18	A2B5	VWM	F	0.070	0.221	81	71
19	A2B5	VWM	F	0.098	0.224	80	86
20	GLAST	VWM	M	0.084	0.302	82	70
21	GLAST	VWM	M	0.147	0.334	67	68
22	GLAST	VWM	F	0.091	0.155	98	82
23[g]	**GLAST**	**VWM**	**F**	**0.034**	**0.173**	**89**	**75**
24	GLAST	VWM	F	0.121	0.280	57	59
25	GLAST	VWM	F	0.115	0.248	74	74
26	PDGFαR	VWM	F	0.102	0.149	72	64
27	PDGFαR	VWM	M	0.143	0.189	76	78
28	PDGFαR	VWM	M	0.132	0.204	90	79
29[g]	**PDGFαR**	**VWM**	**M**	**0.040**	**0.160**	**95**	**77**
30[g]	**PDGFαR**	**VWM**	**F**	**0.065**	**0.175**	**92**	**87**

[a] Saline = saline injected mice; A2B5, GLAST and PDGFαR = mice injected with primary mouse cells sorted on marker expression of the named proteins.

[b] Genotype of mice: WT = wildtype, VWM = VWM mice,

[c] Ratio of Nestin$^+$ cells to total number of DAPI$^+$ cells in the corpus callosum

[d] BG = Bergmann glia. Ratio of translocated Bergmann glia to total number of Bergmann glia

[e] cc = corpus callosum. Average number of *Plp*$^+$ cells in a 100x200 micron square in the corpus callosum

[f] cer = cerebellum. Average number of *Plp*$^+$ cells in a 100x200 micron square in the cerebellum.

[g] Bold script indicates transplanted animals that were classified as WT in the discriminant analysis.

Table S2. Injection coordinates for cell transplantation in P0 pups.

Weight of pup	Injection site	X[a]	Y[b]	Z[c]
0.9 gr	Posterior corpus callosum	±1.4	0	-.5
	Anterior corpus callosum	±0.9	-2	-.4
	Cerebellum	±1.1	1.9	-1.5
1.0 gr	Posterior corpus callosum	±1.4	0	-.5
	Anterior corpus callosum	±1	-2.1	-.4
	Cerebellum	±1.1	2	-1.5
1.1 gr	Posterior corpus callosum	±1.4	0	-.5
	Anterior corpus callosum	±1	-2.2	-.4
	Cerebellum	±1.2	2	-1.5
1.2 gr	Posterior corpus callosum	±1.6	0	-.5
	Anterior corpus callosum	±1.1	-2.2	-.5
	Cerebellum	±1.2	2.1	-1.6
1.3 gr	Posterior corpus callosum	±1.6	0	-.6
	Anterior corpus callosum	±1.1	-2.3	-.5
	Cerebellum	±1.2	2.1	-1.7
1.4 gr	Posterior corpus callosum	±1.6	0	-.6
	Anterior corpus callosum	±1.2	-2.3	-.5
	Cerebellum	±1.2	2.2	-1.7
1.5 gr	Posterior corpus callosum	±1.6	0	-.7
	Anterior corpus callosum	±1.2	-2.4	-.5
	Cerebellum	±1.2	2.2	-1.8
1.6 gr	Posterior corpus callosum	±1.6	0	-.7
	Anterior corpus callosum	±1.3	-2.4	-.6
	Cerebellum	±1.3	2.3	-1.8
1.8 gr	Posterior corpus callosum	±1.6	0	-.7
	Anterior corpus callosum	±1.3	-2.4	-.6
	Cerebellum	±1.3	2.3	-1.8

[a,b,c] The coordinates are in mm distance to the lambda, which is clearly visible in P0 pups.

[a] The X-coordinates represent the medial-lateral or left-right plane.

[b] The Y coordinates represent the rostral-caudal or front-back plane.

[c] The Z coordinates represent the ventral-dorsal or up-down plane.

Supplemental Experimental Procedures

Experimental animals
For this study mice with a homozygous mutation in the *Eif2b5* gene were used (*Eif2b5*$^{R191H/R191H}$; called *2b5*^{ho} or VWM mice, background strain C57Bl/6J (Dooves et al., 2016)). Littermates with heterozygous *Eif2b5* mutations were used as WT animals for the transplantation experiments as these mice do not show any disease phenotype. For cell sortings WT C57Bl/6J mice were used. Untreated *2b5*^{ho} mice show astrocytic abnormalities from P14 onwards, followed by myelin abnormalities from 1 month of age and ataxia from 4 months of age. Between 7 and 10 months of age untreated *2b5*^{ho} mice reach their humane endpoint, defined as the moment they become unable to take food or water or when they lost more than 15% of their body weight (Dooves et al., 2016). Pups were injected with cells or saline at postnatal day 0 (P0) as described below. Pups were weaned at P28 and housed in groups separated by sex.

Mice were sacrificed at 2 months, 5 months and 9 months of age by transcardial perfusion with 4% paraformaldehyde. Half of the brain was post-fixed for 24h, cryoprotected in 30% sucrose overnight and snap-frozen in Optimal Cutting Temperature mounting medium (Sakura Finetek Europe BV). The other half was embedded in paraffin. For every age group and experimental group 5-10 *2b5*^{ho} animals were collected: WT saline (9m n=11), VWM saline (9m n=22), VWM A2B5 (2m n=5, 5m n=5, 9m n=8), VWM GLAST (2m n=5, 5m n=5, 9m n=6), VWM PDGFαR (2m n=6, 5m n=5, 9m n=5). Due to differences in litter size and number of homozygous mutant animals per litter, the group sizes were slightly different for each condition. All mouse procedures were carried out according to the guidelines of the Dutch government and approved by the Animal Approval Committee of the VU University Amsterdam.

Motor tests
The motor skills of mice were tested at 7 months of age on WT saline (n=11), VWM saline (n=22), A2B5 injected (n=8), GLAST injected (n=6) and PDGFαR injected (n=5) mice. On the balance beam test, mice were trained to run over a narrow beam into an enclosed box. The number of slips and the time it took them to cross the beam were recorded. The grip strength meter was used to measure the strength of the front paws and the front and hind paws combined, by pulling mice over a grid that records the strength that mice use to hold on to the grid. The footprint test was used to analyse gait ataxia. The front paws of the mice were painted with red ink, and the hind paws with blue ink. Mice were then allowed to run over a paper. Papers were later scanned and gait parameters like stride length and gait width were recorded. See (Dooves et al., 2016) for more information.

Primary cell isolation
Forebrains from embryonic day 18 WT pups were dissociated with the GentleMACS dissociater (Miltenyi Biotec) as previously described (Dooves et al., 2016). After overnight recovery on an anti-adhesive plate, different cell populations were sorted with magnetic activated cell sorting (MACS) according to manufacturers' protocol (Miltenyi Biotec). Different glial progenitor populations were sorted for marker expression of A2B5, GLAST or PDGFαR. After the sorting cells were transduced by centrifuging for 1 hr at 37°C at 600 g in DMEM/F12 supplemented with polybrene (10 µg/ml) and GFP lentivirus. After transduction cells were washed with PBS twice and resuspended as $1x10^5$ cells per 400 nl in saline with DNAse (100 µg/ml) and immediately used for cell transplantation.

Production of lentivirus
A lentiviral GFP plasmid (LV-PGK-eGFP) was kindly gifted by Joost Verhaagen (Netherlands Institute for Neurosciences, Amsterdam, The Netherlands). Virus was produced by transfecting the plasmid and packaging plasmids (ViraPower™ Packaging Mix, Invitrogen) with FuGene in serum free opti-MEM medium in HEK293T cells overnight. The next day medium was replaced with serum free opti-MEM for virus collection. Medium was collected on two consecutive days. Virus-containing medium was concentrated by spinning down for 3 hr at 20.000 rpm. Afterwards, most of the supernatant was removed leaving about 200 µl of medium. The virus was resuspended by incubating on ice on a rocking platform for 1 hour, aliquoted and stored at -80°C. For every new virus batch the amount of virus needed to reach an ~70-80% transduction efficiency was tested on primary dissociated cells.

Cell injections
Pups were sedated before injections by incubation on ice for 7 min. Clay holders were used to keep pups in place under the stereotact. These clay holders were made by pressing (sedated) pups with different body weight in ~37°C warm low-melting-temperature agarose to make an impression of the pup. The agarose was cooled in the fridge until it was hard and filled with clay to make a clay pup. This clay pup was baked and pressed in clay to make a clay

holder. These clay holders were baked, marked with the pups weight and used for injections for pups of similar weight. Cells were stereotactically injected bilaterally in the anterior corpus callosum, posterior corpus callosum and the cerebellum. The injection coordinates used can be found in Table S2. It is important to note that the exact coordinates needed to target these specific areas will differ when the pup is placed underneath the stereotact at a different angle. For this reason, this coordinates are useful with the exact clay holders used in this study, and will need to be optimized on other setups. Per injection site $1x10^5$ cells were injected in a volume of 400 nl. Control animals got the same injections but with 400 nl saline. After injections pups were put on a heating mat for a few minutes until they were awake, and returned to their mother.

In vitro cell analysis

To analyse *in vitro* differentiation patterns cells were isolated from E18 mice in 3 independent experiments and sorted for marker expression of A2B5, GLAST or PDGFαR as described above. After sorting, cells were not transduced with GFP virus but immediately lysed in TRIzol® (Life Technologies) to extract RNA or plated at 100.000 cells/well on a PLO/laminin coated 8 well chamberslide in M41 medium (medium was refreshed after 3 days). Cells were fixed at 1 day and 1 week after sorting by incubation in 2% PFA for 20 min. Immunostaining on cell culture was performed as described below, but without the citrate buffer antigen retrieval step. Antibodies used targeted GFAP (1:1000, Sigma-Aldrich, G3893), OLIG2 (1:500, Millipore, AB9610), SOX9 (1:250, Cell Signalling, 82630), PDGFαR (1:250, eBioscience, 13-1401-82), MAP2 (1:20000, Abcam, AB5392) and CD11b (1:50, developed by Springer T.A. and obtained via the Developmental Studies Hybridoma Bank, M1/70.15.11.5.2). For cell counts 10 random pictures per well were taken. For each marker the number of positive cells as a percentage of the total number of $DAPI^+$ cells was calculated. Contamination of MAP2+ and $CD11b^+$ cells was lower than 5% after sorting.

RNA was isolated by chloroform separation and precipitated with isopropanol. RNA concentrations and purity (260/280 and 260/230 values) were measured on a Nanodrop (Thermo Scientific) and cDNA was synthesized from 950 ng RNA with random hexamer primers. For qPCR cDNA samples were diluted 30 times and qPCR was performed with SensiFast Sybr Hi-ROX-kit (GC Biotech) on a Lightcycler480 (Roche) according to manufacturer's protocol. All reactions were performed in duplo. Primers were targeting housekeeping genes *Gapdh* (forward GTGCTGAGTATGTCGTGGAG; reverse TCGTGGTTCACACCCATCAC) and 18S (forward TTCTCGATTCCG TGGGTG; reverse GCGTAACTAGTTAGCATGCC) or target genes *Gfap* (forward AAGCCAAGCACGAAGCTA ACGA; reverse TTGAGGCTTTGGCCCTCC), *Olig2* (forward TGTGGATGCTTATTACAGACC; reverse ATCTAAGCTCTCGAATGATCC), *Glast* (forward TGTCATTGTGGGTACAATCCT; reverse ACAGCAATGAT GGTAGTAGTC), *Pdgfra* (forward CCGGGCTAAGGAAGAAGAC; reverse ATGCAGGAACTAGGGTTGAC), *Ngf1* (forward ACTTCCAGGCCCATGGTACAATCT, reverse TTGATGTCCGTGGCTGTGGTCTTA), *Nt3* (forward ACTACGGCAACAGAGACGCTACAA, reverse ATAGCGTTTCCTCCGTGGTGATGT), *Pdgfa* (forward CCAGCGACTCTTGGAGATAGAC, reverse GAATGGCTTCCTCAATACTTCTCT), *Egf* (forward CTG GACAGACAGTGGGAAGTC, reverse CGTCCGTCCAGAACAGTCTC), *Lif* (forward TGCCAATGGGACAGA GAAGACCAA, reverse TACTTGTTGCACAGACGGCAAAGC), *Igf1* (forward TGGCACTCTGCTTGCTCAC CTTTA, reverse TTGGTCCACACACGAACTGAAGAG), and *Tgfβ* (forward ACTGGAGTTGTACGGCAGTG, reverse GGCTGATCCCGTTGATTTCC). Primer sequences for *Ngf1*, *Nt3*, *Lif* and *Igf1* are obtained from Hawryluk et al. (2012). Data was analysed according to the $2^{-\Delta CT}$ method, using housekeeping CT values and target CT values per sample to calculate ΔCT values.

Immunohistochemistry and cell counts

Fluorescent immunostainings were performed on snap-frozen brain sections. Sagittal brain sections were cut on a Leica CM 1950 cryostat (Leica Microsystems) in 12 µm thickness and in series of 12 slides with 3-6 brain sections per slide. The number of brain sections was the same for all slides within each series of 12 slides, and within one series first one brain section is added on all slides, before proceeding with the second brain section on each slide. This way of cutting ensures that all slides within one series are from similar lateral distances.

For immunostaining slides were washed with PBS for 30 min and treated with citrate buffer at 90°C for 10 min to retrieve antigens. After cooling down, sections are incubated in blocking solution (PBS+ 5% normal goat serum + 0.1% bovine serum albumin + 0.3% Triton X-100) for 1 hour and incubated in primary antibody diluted in blocking solution overnight at 4°C. The next day, slides are washed for 30 min in PBS and incubated in secondary

antibody (Alexa Fluor 488- , Alexa Fluor 594-, or Alexa Fluor 647-tagged secondary antibodies; 1:1000, Fisher Scientific) in blocking solution for 2 hours at room temperature (RT). Pictures were taken with a Leica DM6000B microscope (Leica Microsystems). Brightness and contrast was optimized using Adobe Photoshop CS6. Antibodies used targeted GFP (1:500, Aves Labs, GFP-1020), GFAP (1:1000, DAKO, Z0334), OLIG2 (1:500, gift of J.H. Alberta, Harvard University, Boston, Massachusetts, USA), Nestin (1:500, BD Biosciences, 611658) and S100β (1:1000, ProteinTech, 15146-1-AP).

For Nestin cell counts, tissue sections were stained with Nestin and GFAP primary antibodies. All pathology measurements were performed on 9 months old mice of all groups: WT saline (n=4), VWM saline (n=7), A2B5 cells (n=8), GLAST cells (n=6) and PDGFαR cells (n=5) injected mice. Per animal at least 6 pictures of 100x magnification of the rostrum and splenium of the corpus callosum were taken. On each picture, the number of $Nestin^+/GFAP^+$ cells were counted, and expressed as a ratio to the total number of $DAPI^+$ nuclei.

Bergmann glia translocation was assessed with S100β staining. All pathology measurements were performed on 9 months old mice of all groups: WT saline (n=4), VWM saline (n=7), A2B5 cells (n=8), GLAST cells (n=6) and PDGFαR cells (n=5) injected mice. For each animal, at least 6 pictures of the cerebellum at 100x magnification were taken, all including the Purkinje cell layer and the molecular layer. With ImageJ software (NIH) the number of $S100\beta^+$ cell bodies in the Purkinje cell layer and the molecular layer were quantified as described previously (Dooves et al., 2017). The number of $S100\beta^+$ cell bodies in the molecular layer were considered translocated, and were expressed as the ratio of translocated cell bodies to the total number of $S100\beta^+$ cell bodies in the Purkinje cell layer and the molecular layer.

To analyse cell survival and cell fate one slide from each series of 12 slides was stained for GFP expression. The total number of engrafted cells was estimated in one hemisphere per animal based on counts of GFP+ cells in different brain sections. On each slide the number of GFP^+ cells per brain area was quantified. To estimate the total amount of GFP^+ cells present the total number of counted cells was multiplied by 12. This gives an estimation of the number of cells present in half of the brain. One brain half receives 3 injections of 100.000 cells, so 300.000 cells of which about 70-80% is GFP^+, so about 225.000 GFP^+ cells per brain half are injected. This amount is used to calculate the percentage of engrafted cells (# of GFP^+ cells divided by the # of injected cells). Cell survival was analysed in 2, 5 and 9 months old animals that received injections with A2B5 (2m n=4, 5m n=4, 9m n=5), GLAST (2m n=3, 5m n=5, 9m n=3) or PDGFαR (2m n=6, 5m n=5, 9m n=5) sorted cells.

To analyse cell fate pictures of GFP^+ cells were taken in the cortex (which contains transplanted cells in practically all animals). On each picture the total amount of GFP^+ cells was counted, as well as the number of $OLIG2^+/GFP^+$ and $GFAP^+/GFP^+$ cells. The cell fate is expressed as the ratio of $OLIG2^+/GFP^+$ or $GFAP^+/GFP^+$ cells over the total amount of GFP^+ cells. At least 50 cells were counted per mice. Cell fate was analysed in 2, 5 and 9 months old animals that received injections with A2B5 (2m n=4, 5m n=3, 9m n=4), GLAST (2m n=3, 5m n=4, 9m n=3) or PDGFαR (2m n=5, 5m n=5, 9m n=5) sorted cells.

In situ hybridization and cell counts

Tissue sections were probed against *Plp* mRNA as described previously (Dooves et al., 2016). The dig-labelled *Plp* probe was incubated overnight in hybridization buffer on tissue sections that were pre-treated with proteinase K. Anti-digoxygenin-AP (1:2000, Roche) was used to target the *Plp* probe and the staining was developed overnight with BM Purple (Roche). Nuclei were counterstained with 0.5% methylgreen at 60°C for 5 minutes. All pathology measurements were performed on 9 months old mice of all groups: WT saline (n=4), VWM saline (n=7), A2B5 cells (n=8), GLAST cells (n=6) and PDGFαR cells (n=5) injected mice. Pictures at a 100x magnification were taken of the white matter of the cerebellum and the corpus callosum. The total number of *Plp*-expressing cells was counted in a 100 x 200 µm rectangle. Per animal at least 6 fields per area were counted.

Statistical analysis

All data was analysed using SPSS software (IBM SPSS Statistics 20.0). A Shapiro-Wilk test was performed to test normal distribution of the data. Besides the count of cells *in vitro* after sorting, all data was normally distributed. Counts of cells *in vitro* were analysed with a Mann-Whitney U test. QPCR analysis of cells *in vitro,* cell fate *in vivo* and cell survival *in vivo* were analysed with an ANOVA and post-hoc Tukey test. A MANOVA was used to analyse the different treatment groups on all disease markers. Next a discriminant analysis was used to cluster saline WT and *2b5*^{ho} animals based on the different cell counts. The Box's M test was not significant, suggestion equality of the variance-covariance matrix, showing that the data met the assumptions of the discriminant analysis (normally distributed and equal variance/covariance matrixes). All disease markers had a significant mean difference between WTsal and VWMsal and were included as predictor variables, leading to a highly significant discriminant function that explained 95.1% of the variability ($p<.001$) and could classify all saline-injected animals correctly as WT or

VWM. The formula found in the discriminant analysis was then applied to all transplanted animals to cluster them either with the WT or the *2b5*^{ho} group.